Since January 2020 Elsevier has created a COVID-19 resource centre with free information in English and Mandarin on the novel coronavirus COVID-19. The COVID-19 resource centre is hosted on Elsevier Connect, the company's public news and information website.

Journal of Colloid and Interface Science 592 (2021) 156–166

Contents lists available at ScienceDirect

Journal of Colloid and Interface Science

journal homepage: www.elsevier.com/locate/jcis

Regular Article

Multidomain drug delivery systems of β-casein micelles for the local oral co-administration of antiretroviral combinations

Prakram Singh Chauhan [a], Inbal Abutbul Ionita [a], Hen Moshe Halamish [b], Alejandro Sosnik [b], Dganit Danino [a,c,*]

[a] CryoEM Laboratory of Soft Matter, Faculty of Biotechnology and Food Engineering, Technion-Israel Institute of Technology, Haifa 3200003, Israel
[b] Laboratory of Pharmaceutical Nanomaterials Science, Department of Materials Science and Engineering, Technion-Israel Institute of Technology, Haifa 3200003, Israel
[c] Guangdong Technion – Israel Institute of Technology, Shantou, Guangdong Province 515063, China

GRAPHICAL ABSTRACT

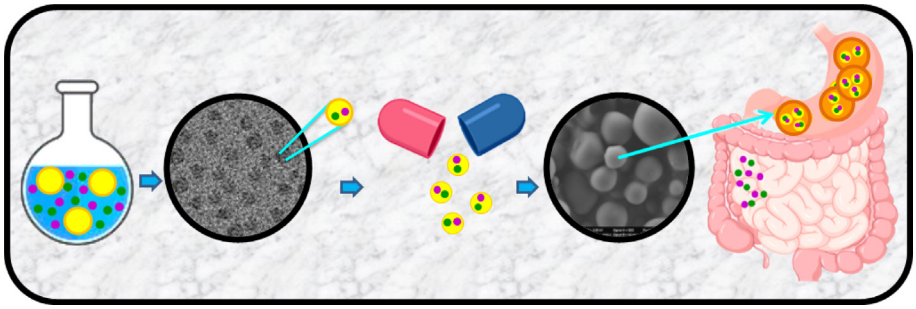

ARTICLE INFO

Article history:
Received 31 August 2020
Revised 20 November 2020
Accepted 8 December 2020
Available online 1 January 2021

Keywords:
Combination therapy
Antiretrovirals
Darunavir, efavirenz and ritonavir
β-casein micelles (bCN)
Colloidal dispersion
cryo-TEM
Nanoparticle-in-microparticle delivery system (NiMDS)

ABSTRACT

The antiretroviral (ARV) cocktail revolved the treatment of the human immunodeficiency virus (HIV) infection. Drug combinations have been also tested to treat other infectious diseases, including the recent coronavirus disease 2019 (COVID-19) outbreak. To simplify administration fixed-dose combinations have been introduced, however, oral anti-HIV therapy still struggles with low oral bioavailability of many ARVs. This work investigated the co-encapsulation of two clinically relevant ARV combinations, tipranavir (TPV):efavirenz (EFV) and darunavir (DRV):efavirenz (EFV):ritonavir (RTV), within the core of β-casein (bCN) micelles. Encapsulation efficiency in both systems was ~100%. Cryo-transmission electron microscopy and dynamic light scattering of the ARV-loaded colloidal dispersions indicate full preservation of the spherical morphology, and x-ray diffraction confirm that the encapsulated drugs are amorphous. To prolong the physicochemical stability the formulations were freeze-dried without cryo/lyoprotectant, and successfully redispersed, with minor changes in morphology. Then, the ARV-loaded micelles were encapsulated within microparticles of Eudragit® L100, which prevented enzymatic degradation and minimized drug release under gastric-like pH conditions *in vitro*. At intestinal pH, the coating polymer dissolved and released the nanocarriers and content. Overall, our results confirm the promise of this flexible and modular technology platform for oral delivery of fixed dose combinations.

* Corresponding author at: CryoEM Laboratory of Soft Matter, Faculty of Biotechnology and Food Engineering, Technion-Israel Institute of Technology, Haifa 3200003, Israel.
E-mail addresses: Danino@Technion.ac.il, Dganit.Danino@GTIIT.edu.cn (D. Danino).

https://doi.org/10.1016/j.jcis.2020.12.021
0021-9797/

1. Introduction

The Human immunodeficiency virus (HIV-1) infection is one of the major health burdens worldwide with approximately 37.9 million people living with HIV in 2018 [1]. An estimated 1.7 million individuals worldwide became newly infected with HIV in 2018 – about 5,000 new infections per day, as well as 940,000 people that died of HIV that year [1]. Different antiretroviral (ARV) combinations have been clinically trialed. Based on clinical evidence, the chronic administration of a minimum of three ARVs of at least two different families (out of the existing six) is critical to maintain undetectable viral levels in plasma over time and to prevent the progress from the infection to the active phase of the disease, the Acquired Immunodeficiency Syndrome (AIDS) [2,3]. The ARV cocktail known as the highly active antiretroviral therapy (HAART) revolutionized the treatment of the disease, making it manageable and chronic. The rationale behind HAART is that the inhibition of the HIV replication cycle at least at two different stages results in therapeutic synergy. More recently, the clinical use of ARV combinations has been implemented in pre-exposure prophylaxis and to prevent HIV infection in non-infected individuals at very high risk. ARV combinations have been also clinically assessed in the treatment of viral diseases such as the severe acute respiratory syndrome (SARS) and lately in the corona virus 2019 (COVID-19) outbreak [4–6]. In late March 2020, the World Health Organization (WHO) launched the global clinical trial called SOLIDARITY comprising several thousands of patients worldwide that aims to find a possible treatment for this new disease [7]. In this framework, the efficacy of the lopinavir/ritonavir (LPV/RTV) combination to prevent infection or improve clinical outcomes will be assessed.

Pill burden and complex administration regimens jeopardize patient compliance and may lead to low therapeutic efficacy due to poor adherence. Fixed-dose combinations (FDCs) are pharmaceutical products containing two or more active pharmaceutical ingredients (APIs) in one single dosage form. FDCs have been designed to reduce pill burden, simplify administration regimens, improve patient compliance, and constrain the risk of monotherapy-associated drug resistance [8]. There are more than 10 2-in-1 and 3-in-1 ARV FDCs approved by the US-Food and Drug Administration (US-FDA) [9]. The non-nucleoside reverse transcriptase inhibitor efavirenz (EFV) and the protease inhibitors darunavir (DRV) and tipranavir (TPV) are among the ARVs approved by the FDA and the European Medicines Agency (EMA) (Fig. 1). EFV [10] is a first-line ARV listed in the WHO Model List of Essential Medicines [11]. DRV is also a first-line drug listed as essential by the WHO, [11] while TPV is second-line due to severe side-effects, though still used in patients that have shown resistance to other protease inhibitors [12]. Protease inhibitors are always associated with a boosting agent such as RTV, taken in low dose [13]. A more selective boosting agent, cobicistat, was introduced in FDCs in 2012 [14]. RTV and cobicistat show similar efficacy [15] but different side effects [16] with limited clinical data for the latter in high-risk subpopulations [17]. Cobicistat-containing FDCs are more costly than those of RTV and less affordable in developing countries [18]. RTV (but not cobicistat) is catalogued by the WHO as an essential drug [11].

EFV, DRV and TPV are classified into Class II of the Biopharmaceutics Classification System (BCS), displaying low water solubility, high permeability and low oral bioavailability [17]. Conversely, RTV belongs to Class IV (low water solubility and low permeability) (Table S1). EFV displays low water solubility in a broad pH range between 1 and 8 and limited oral bioavailability [19]. Protease inhibitors are highly soluble in acid aqueous solutions [20] and present a dramatic solubility decrease at neutral or basic pH. For example, the water solubility of RTV decreases from 1.2 mg mL^{-1} at pH 1 to 5 mg mL^{-1} at neutral pH [21]. Thus, even if administered in the form of water-soluble salts or solvates, protease inhibitors precipitate in the small intestine in the form of relatively large particles with slow dissolution rate, a phenomenon that result in low oral bioavailability [22,23]. In this context, the investigation of advanced drug delivery systems that localize the delivery in the gut is called for, to improve the efficacy and the quality of life of patients and to reduce the medication costs in the therapy of HIV [24–26].

Beta-casein (bCN, 24 kDa, 209 amino acids) is an unstructured calcium-sensitive phosphoprotein, comprising about 36% of the cow milk [27,28]. The most advantageous feature of bCN is its amphiphilic structure that leads to self-assembly in aqueous solution, thereby forming stable colloidal micellar structures [27,29,30]. The monomer radius of gyration (R_g) ranges between 7.3 and 13.5 nm [27,28] depending on temperature, pH, and ionic strength. The critical micellar concentration (CMC) of bCN also depends on these parameters, and at pH 7.0 and the temperature interval relevant to this study it is between 0.5 and 2.0 mg mL^{-1} [28]. In our earlier studies, we showed that bCN micelles can efficiently encapsulate and orally deliver high amount of hydrophobic therapeutics such as celecoxib and except that becoming more round, and importantly no change in the morphology of the micelles occur even after freeze- drying and resuspension [29–31].

The oral route has been recognized as the most patient-compliant, mainly owing to the minimal invasiveness, painless self-administration and possible use of solid formulations with better physicochemical stability and long shelf life and the ability to sustain and localize the release in different portions of the gastrointestinal tract (GIT) [32]. Micelles are common and accepted colloidal particles in drug delivery, and bCN micelles emerge as a versatile, biocompatible platform for oral drug delivery. However, they undergo degradation in the harsh acidic conditions of the gastric fluids (pH 1–2.5) [33], a process that is catalyzed by gastric enzymes such as pepsin [34].

Aiming to make a sound contribution to the combined ARV therapy of HIV and pave the way for the use of bCN micelles in oral drug delivery, in this work we investigated and characterized a Nanoparticle-in-Microparticle Drug Delivery System (NiMDS) 2-in-1 and 3-in-1 FDCs to improve the oral bioavailability and reduce the administration frequency of ARVs. Our results demonstrate the promise of these modular and versatile delivery constructs for the local oral delivery of ARV FDCs in the therapy of HIV and possibly other viral infections.

2. Materials and methods

2.1. Production of drug-loaded bCN dispersions

Bovine bCN (>97% purity, Sigma-Aldrich) was dissolved in 50 mM phosphate buffered saline (PBS, pH 7.0, MP Biomedicals) containing 5.65 mM NaH_2PO_4 (99% purity, Merck Millipore), 3.05 mM Na_2HPO_4 (99% purity, Merck Millipore), 80 mM NaCl (98% purity, Loba Chemie) and 0.02% sodium azide (≥99.5% purity, Sigma-Aldrich). The bCN colloidal system was prepared at 10 mg mL^{-1} (0.41 mM), above its CMC (0.5–2.0 mg mL^{-1}, 0.021–0.083 mM at pH 7.0, 25 °C), where physically stable bCN micelles exist [28,29]. The system was stirred overnight at 4 °C, forming a transparent colloidal dispersion.

For loading bCN micelles with TPV (≥98% purity, MW of 602.66 g mol^{-1}, Boehringer Ingelheim) and EFV (≥98% purity, MW of 315.67 g mol^{-1}, Gilead Sciences), the drugs were dissolved in absolute alcohol (Bio-Lab Ltd.). For the preparation of bCN micelles loaded with DRV (98% purity, MW of 547.66 g mol^{-1}, Leap Chem Co.), EFV and RTV (99% purity, MW of 720.94 g mol^{-1}, Leap Chem Co.), they were dissolved in dimethyl sulfoxide (≥99% purity,

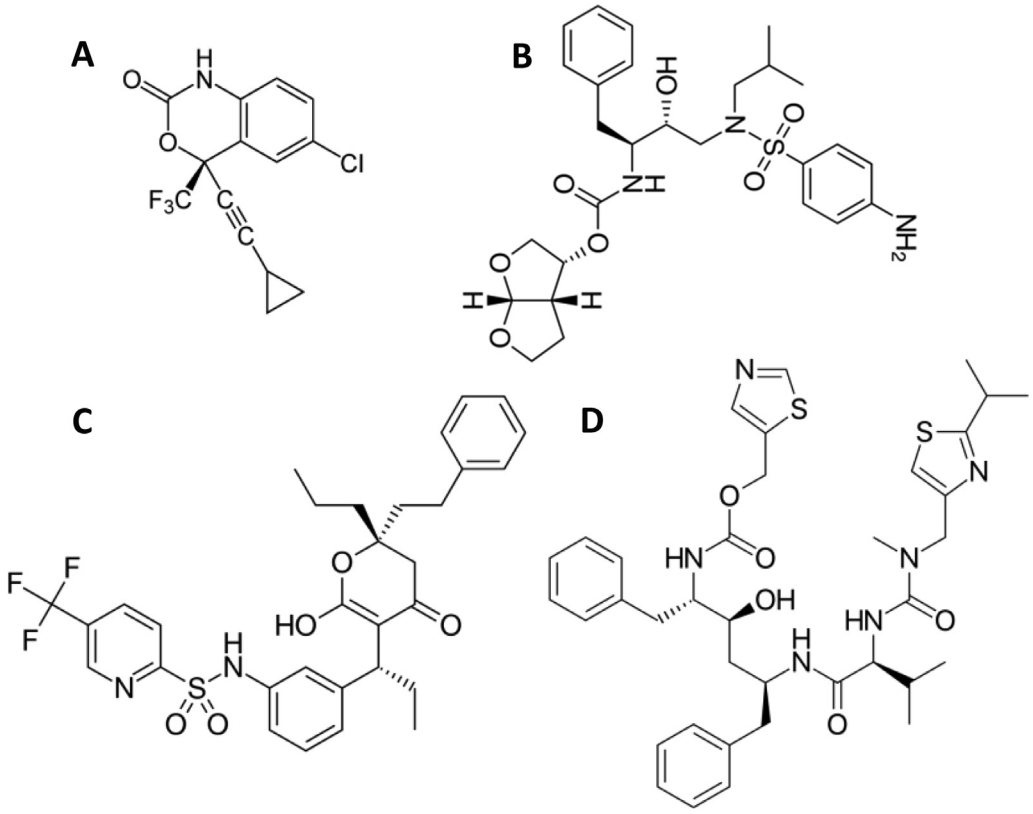

Fig. 1. Chemical structure of (A) EFV, (B) DRV, (C) TPV and (D) RTV.

DMSO, Bio-Lab Ltd.). As controls, each drugs mixture - TPV:EFV in ethanol (99% purity, Parchem) or DRV:EFV:RTV in DMSO - was added dropwise to PBS. All control drug dispersions were cloudy, indicating poor dispersibility and poor solubility of the drugs in buffer.

For the dispersion, a known amount of each drugs mixture was added dropwise to bCN micelles (10 mg mL^{-1}) under stirring for 30 min at 25 °C, at predetermined protein:drugs mole ratios. Ethanol or DMSO concentration in the final dispersion was always <5% v v^{-1}. The drug-loaded dispersion bCN:TPV:EFV is designated as bCTE (1:8:8 protein:drugs mole ratio) and bCN:DRV:EFV:RTV is designated bCDER (1:8:6:1 protein:drugs mole ratio), and compositions are given in Table 1. All of these dispersions were transparent indicating good encapsulation of the drugs within the micelles.

Drug-loaded bCN micelles were encapsulated within Eudragit® L100 (Evonik) using direct Nano Spray-Drying (see below) to form gastro-resistant microparticles that are fully stable under gastric pH conditions and dissolve fast at pH = 6–7 (small intestine). To confirm the copolymer coating of the micelles, an acidic protease solution from *Aspergillus saitoi* (0.6 U mg^{-1}; Sigma-Aldrich) was used to challenge their stability *in vitro*.

2.2. Freeze-drying

The drug-free and drug-loaded bCN colloidal dispersions were frozen in liquid nitrogen and then freeze-dried in an Alpha 1–4 LSC basic lyophilizer (Martin Christ) for 24 h. Samples were stored at 4 °C, then resuspended in PBS, to reach the original concentration of 10 mg mL^{-1}, or a higher concentration of 50 mg mL^{-1}. Resuspension was performed by weighing the dry powder, adding a measured volume of PBS, and stirring for 30 min at room temperature. Transparent dispersions were obtained.

2.3. Turbidity

Turbidity measurements were performed using an Ultrospec 2100 Pro spectrophotometer (Amersham Biosciences Corp.) at a wavelength of 600 nm with a light path of 1 cm. bCTE and bCDER dispersions at predetermined molar ratios were characterized.

2.4. Characterization of drug-loaded bCN dispersions

The size distribution (scattering angle of 173°) and zeta-potential (Z-potential) were measured by dynamic light scattering (DLS) in a Zetasizer Nano ZSP (Malvern Panalytical Ltd.) at 25 °C. Z-potential of bCTE and bCDER was measured before freeze-drying, and after resuspension in PBS. An Olympus BX51 light microscope (LM, Olympus Corp.) was operated at Nomarski differential interference contrast (DIC) optics to examine the drugs in PBS and drug-loaded bCN dispersions. One drop (5 μL) was placed on a glass slide and covered with a cover slide. Images were recorded digitally at magnifications of 10- to 60-fold, with an Olympus DP71

Table 1
Composition of different formulations used in this study.

	bCN:TPV:EFV			Total amount (mg)	bCN:DRV:EFV:RTV				Total amount (mg)
Component	bCN	TPV	EFV		bCN	DRV	EFV	RTV	
Amount (mg)	10	1.90	0.99	12.9	10	1.7	0.74	0.28	12.7

camera connected to the LM. Image processing was done using the Cell A software (Olympus Corp.).

2.5. Direct-imaging cryogenic-transmission electron microscopy, Cryo-TEM

Samples for cryo-TEM were prepared in a closed, home-made specimen chamber that was saturated with water and maintained at a controlled temperature (25 °C). A small drop (6 μL) of each colloidal suspension was placed on a 200 mesh carbon-coated copper grid (Ted Pella, Inc.) held by tweezers. Excess sample was removed by blotting with a filter paper to create a thin liquid film filling the holes of the grid of the dispersion of the dispersion. The blotted grids were vitrified upon plunging into the cryogen, liquid ethane maintained at its freezing temperature (−183 °C), transferred to liquid nitrogen (LN2) and then stored in liquid nitrogen (−196 °C) until analysis. Samples were examined in a Tecnai 12 G2 transmission electron microscopy (TEM, FEI) at 120 kV with a Gatan 626 cryo-holder (Pleasanton) maintained below − 170 °C to avoid the crystallization of the vitreous ice. To minimize beam exposure and radiation damage, images were recorded under low-dose conditions to minimize radiation damage on a cooled UltraScan 1000 2 k × 2 k high-resolution charge-coupled device (CCD) camera (Gatan), using the Digital Micrograph software package (Gatan), and using methodologies we have developed, as previously described [35].

2.6. Wide-angle X-ray diffraction, XRD

XRD experiments of freeze-dried bCN, unprocessed drugs, (EFV, TPV, DRV and RTV) and freeze-dried drug-loaded bCN samples (bCTE and bCDER) were performed using a Philips PW 3020 powder diffractometer equipped with a graphite crystal monochromator. The operating conditions were CuKα radiation (0.154 nm), 40 kV and 40 mA, in 2θ recording range from 0° to 90°, at room temperature.

2.7. In vitro pH-dependent dissolution assay

To assess the dissolution and re-precipitation of drugs in PBS media that mimics the pH conditions of the gastrointestinal tract *in vitro*, 2.89 mg of TPV:EFV and 2.75 mg of DRV:EFV:RTV (total drugs amount used for encapsulation) were dispersed in 0.001 M HCl s (pH 2.0, 2.0 mL) at 37 °C and gently stirred at 350 RPM for 30 min. The dispersion was analysed by LM. Then, 5 mM KOH aqueous solution was added to rise the pH from 2.0 to 6.5, and the dispersion was examined again by LM.

2.8. Production and characterization of Nanoparticle-in-Microparticle delivery Systems, NiMDS

NiMDS containing bCTE and bCDER as the nanoparticulate component were produced by the redispersion of the drug-loaded micelles in Eudragit® L100 ethanol solution and spray-drying [36] and designated EbCTE and EbCDER, respectively. Briefly, 50 mg of freeze-dried drug-loaded bCN micelles were dissolved in water and mixed slowly with the copolymer solution prepared in absolute ethanol (5.0 mg mL^{-1}), set the pH solution (7.5) and then spray-dried to form microparticles using a BUCHI B-90 HP Nano Spray Dryer (Flawil) in a closed loop system with the following process setup: 4.0 μm mesh; 80 °C inlet temperature; 22–25 °C outlet temperature; 100 L min^{-1} gas flow rate; 20–25% pump speed; 80% spray power; and 80–90 kHz frequency. As a control, drug-free NiMDSs were produced by dispersing bCN micelles in water and then in Eudragit® L100 solution in absolute alcohol as described above. Microparticles were stored at room temperature until characterization.

Microparticles size and size distribution were assessed after dispersion in 10 mM sodium chloride (25 μg mL^{-1}) using a Zetasizer Nano ZSP, at 25 °C. The size and morphology were further analyzed by scanning electron microscopy (SEM) using a Zeiss Ultra-Plus microscope (Carl Zeiss NTS GmbH). Images were acquired using secondary electrons at 2 keV and at a working distance of 2.5–4.0 mm.

2.9. Fourier-transform infrared spectroscopy, FTIR

To confirm the efficient coating of the micelles with Eudragit® L 100, that is critical to ensure their stability under gastric-like pH conditions, bCN, pristine Eudragit® L 100 and the drug-free bCN microparticles were analyzed by FTIR spectrometry using a Nicolet 6700 FTIR spectrophotometer (Thermo Fisher Scientific,) at scanning range of 4000–500 cm^{-1} and resolution of 2 cm^{-1}.

2.10. Drug release in vitro

The release of DRV, EFV and RTV from the bCDER designated as bCD, bCE, bCR and from EbCDER designated as EbCD, EbCE, EbCR were assessed *in vitro* in both gastric- and intestinal-like pH conditions. Drug-loaded samples (bCDER; 12.75 mg mL^{-1} and EbCDER; 125 mg mL^{-1}) were placed in a dialysis membrane (12–14 kDa MWCO, Spectrum Laboratories Inc.) and immersed in pH 2.0 (lactic acid solution) or pH 6.8 (PBS), at 37 °C, and magnetically stirred at 50 RPM for 48 h. At predetermined time points, release medium aliquots were sampled and replaced by fresh pre-heated medium. Aliquots were freeze-dried and re-dissolved in DMSO. Then, the concentration of each drug was determined by UV–Vis spectrophotometry at 265, 247 and 238 nm respectively, using a calibration curve in DMSO with concentrations up to 1 mg. From this, the cumulative dissolution (expressed in percentage) was calculated. Experiments were conducted in triplicates and results expressed as Mean ± S.D.

2.11. Protection against gastric enzymes

To evaluate the protective effect of Eudragit® L100 against gastrointestinal enzymes under gastric pH conditions, bCDER (12.75 mg mL^{-1} and EbCDER; 125 mg mL^{-1}) were incubated with acidic protease enzyme (6 U) in simulated gastric conditions (pH 2.0, 37 °C) with continuous shaking for 60 min. Samples (500 μL) were taken at every 10 min and centrifuged at 8,000 RPM for 5 min, and supernatant were used for protease activity calculation, knowing that one unit of enzyme hydrolyzes casein to produce color equivalent to 1.0 μmole of tyrosine per min under standard conditions.

2.12. Statistical analysis

Statistical testing was performed by one-way ANOVA for group analysis using GraphPad Prism (GraphPad Software). The results from three independent experiments are presented as mean values ± S.D.

3. Results and discussion

3.1. Production of drug-loaded bCN micelles

NiMDS are comprised of one nanoparticulate and one microparticulate component. Aiming to investigate the potential of bCN micelles to serve as the nanocarrier in ARV NiMDS FDCs for oral drug delivery, we encapsulated one 2-in-1 (TRP:EFV) and one 3-in-1 (DRV:EFV:RTV) drug combination. The former combination is a

prototype used for the optimization of the production process, while the latter is a clinically relevant ARV combination. We first characterized the solubility of these combinations in PBS. As expected, due to their poor solubility in PBS, these drug combinations form large crystals that precipitate with time (Fig. 2A1, A2, B1, B2).

After encapsulation of these hydrophobic ARV combinations within bCN micelles, their aqueous solubility was dramatically increased, resulting in completely transparent dispersions and the absence of drug crystals (Fig. 2C1, *C2*, D1, D2). These results are consistent with the formation of strong interactions between the drug and the hydrophobic domains of the bCN micelles, that result in their efficient encapsulation and the creation of stable drug-loaded bCN dispersions, in agreement with our previous reports for Celecoxib [30,31].

3.2. Characterization of the drug-loaded bCN colloidal dispersions

To evaluate the stability and shelf life of the drug-loaded dispersions, turbidity was measured at selected time points up to ~ 2 weeks (0.5, 1, 24, 48, 96, 120, 144 and 312 h). All dispersions showed good physical stability, and remained clear and transparent over the entire incubation time. The optical density (OD) was 0.08 ± 0.01 and 0.040 ± 0.01, for bCTE and bCDER, respectively. This indicates that the ARV combinations were efficiently retained inside the bCN micelles (Fig. 1S).

Then, we produced dry powders that usually display much higher physicochemical stability and longer shelf life than aqueous liquid dispersions. Superior to many other nanoparticulate drug delivery systems [37], these dispersions could be successfully freeze-dried without the addition of cryo/lyoprotectants, and, in addition, the dry drug-loaded micelles were stable for at least 6 months in the dry form. As shown in Fig. 3, the drug-free bCN colloidal dispersions showed a single narrow peak with an average diameter of 25 ± 2 nm by DLS. Each of bCN-encapsulated dispersions (bCTE and bCDER) showed a single peak as well, yet with larger average diameters of 35 ± 1 nm and 37 ± 3 nm, respectively, before lyophilization and after lyophilization and resuspension to the original concentration in PBS (Table S2). The size growth upon drug encapsulation was consistent with the enlargement of the hydrophobic domains of the micelle, upon drugs encapsulation, as was also found for celecoxib [29]. All the dispersions were transparent to the naked eye before (Fig. 3a1, b1, c1) and after freeze-drying and resuspension (Fig. 3a2, b2, c2). Measurements indicated a slight increase in turbidity for the drug-loaded bCN micelles with respect to the unloaded control, probably owing to the size growth (Fig. 3). Z-potential of all the tested samples remained unchanged (approximately −12 mV) (Fig. 3). These findings highlight the high stability and processability of ARV-loaded bCN micelles, in good agreement with our results with other hydrophobic drugs [30,31]. Remarkably, in this work, double and triple drug combinations were successfully encapsulated with complete preservation of the micellar morphology.

To confirm the efficient drug encapsulation and disclose the micellar morphology, bCTE and bCDER before and after freeze-drying and resuspension were analyzed by cryo-TEM. bCTE micrographs show the presence of a homogenous population of small round and swollen micelles, with a diameter of 21 ± 3 nm (Fig. 4A1) for the fresh dispersion. The size remained almost unchanged after freeze-drying and resuspension (Fig. 4A2). Cryo-TEM images of bCDER showed round micelles of 25 ± 3 nm before (Fig. 4B1) as well as after freeze-drying (Fig. 4B2). The latter are also larger which is consistent with the increased drug loading.

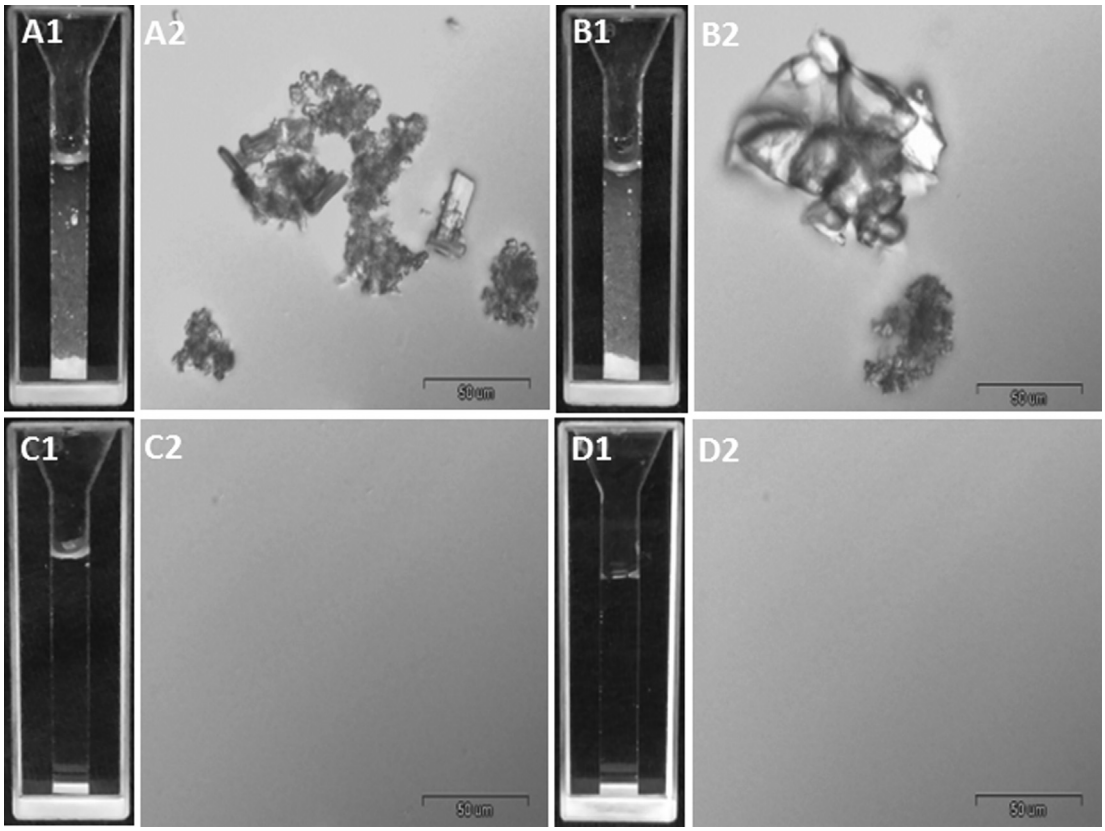

Fig. 2. LM and DIC images showing floating crystals of free drug combinations: (A) TPV:EFV, at 1:1 mol ratio, and (B) DRV:EFV:RTV, at 8:6:1 mol ratio, and complete solubilization after encapsulation in bCN micelle: (C) bCTE, at 1:8:8 protein:drugs mole ratio, and (D) bCDER, at 1:8:6:1 protein:drugs mole ratio. bCN concentration is 10 mg mL^{-1}, and compositions according to Table 1.

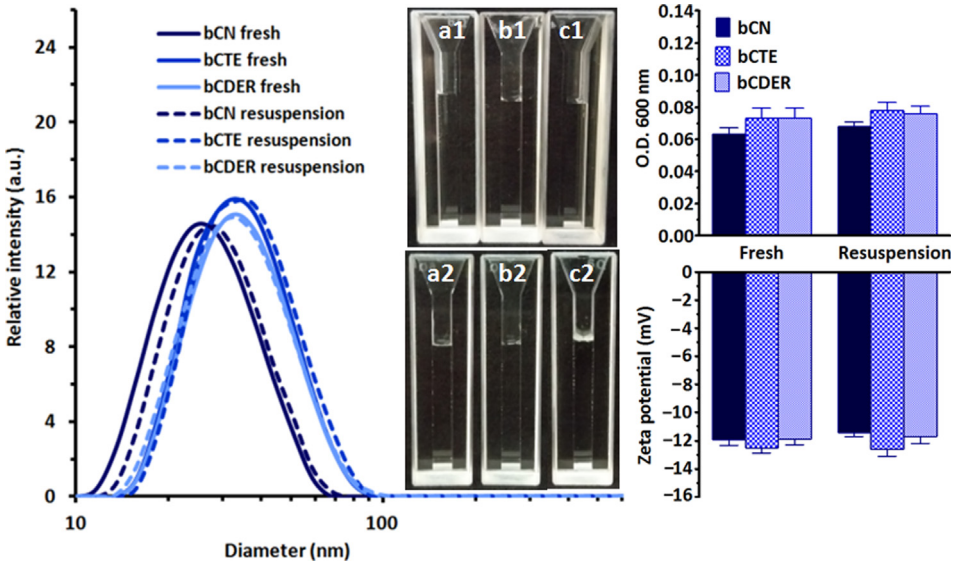

Fig. 3. Right: Size distribution expressed as hydrodynamic diameters, of drug-free and drug-loaded bCN micelles (solid lines), with a mean diameter 25 ± 2 nm growing to 35 ± 1 nm and 37 ± 2 nm after encapsulation. No influence of drying on the mean diameter was observed after resuspension the dry dispersions in PBS to the original compositions (doted lines). The corresponding solutions were transparent both before (a1, b1, c1) and after (a2, b2, c2) lyophilization. Left: Turbidity (upper panel) and Z-potential (lower panel) of drug-free and drug-loaded bCN micelles before and after lyophilization and resuspension shows no change in the overall electro-kinetic potential suggesting good stability of the colloidal dispersion. The results from three independent experiments are presented as mean values ± S.D.

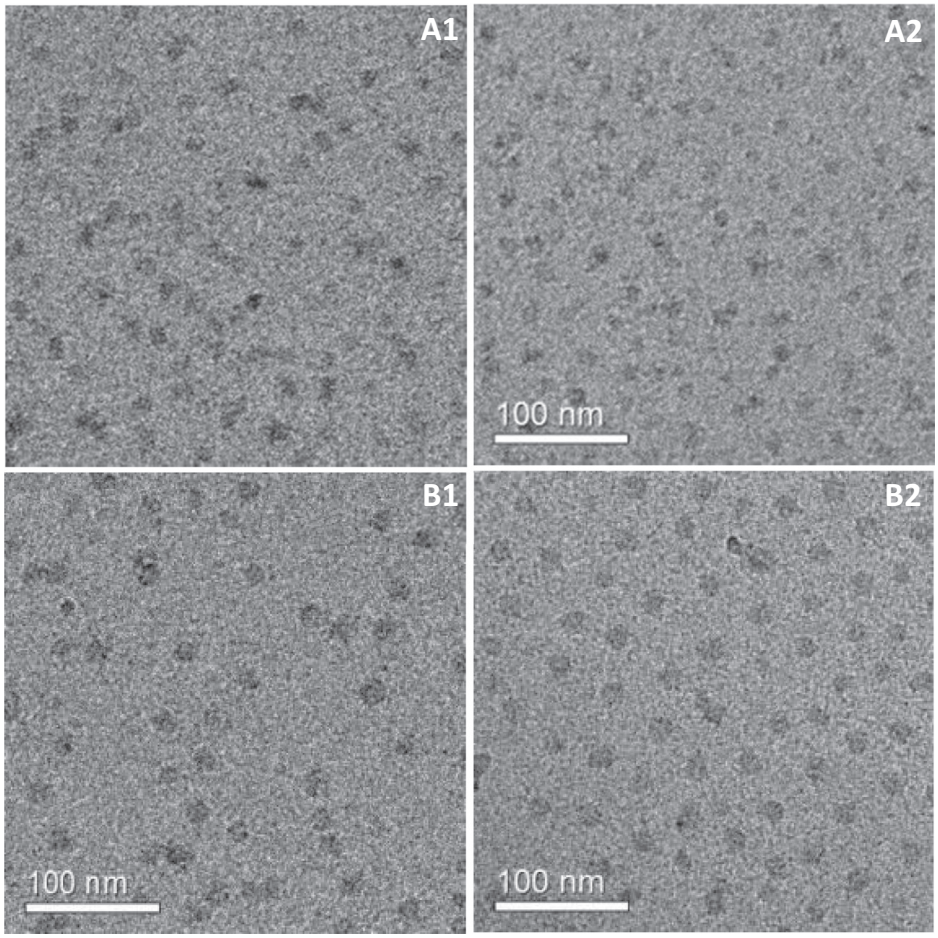

Fig. 4. (A) Cryo-TEM images of bCTE (1:8:8 protein:drugs mole ratio): (A1) fresh and (A2) after freeze-drying and resuspension to the original concentration. (B) Cryo-TEM images of bCDER (1:8:8 protein:drugs mole ratio): (B1) fresh and (B2) after freeze-drying and resuspension to the original concentration.

We further resuspended the freeze-dried bCDER powder in a smaller aqueous medium volume to reach a higher concentration (50 mg mL^{-1}) than the original one. This concentration change might be relevant for the bench-to-bedside translation, as it would enable oral administration of much higher doses in a similar volume. The suspensions remained transparent and the micelles size and morphology remained mostly unchanged (Fig. 5A, B). Sizes measured by DLS were in good agreement with cryo-TEM data [38]. These results together with the absence of crystals at the micro scale (by LM) or the nano-scale (by cryo-TEM) provide solid evidence of successful drug encapsulation. These results support our previous work where we demonstrated encapsulation of a high concentration (~25% $w.w^{-1}$) of the hydrophobic inflammatory drug celecoxib within bCN [29,30]. The present data clearly supports the suitability of bCN micelles for the encapsulation and oral delivery of ARVs. Another advantage of our approach is the ability to resuspend dry powders in much smaller volumes, which increases the drugs concentration (i.e. from 2.75 to 11.00 mg mL^{-1}), making the dispersion clinically feasible and relevant [31].

XRD was performed to EFV, TRP, DRV, RTV and freeze-dried samples of bCN, bCTE and bCDER. Fig. 6 shows that all the pristine drugs are crystalline in nature presenting typical diffraction peaks of small-molecule organic powders. Conversely, upon encapsulation within bCN micelles, no diffraction peaks were detected, indicating that all drugs are in amorphous form or, in other words, molecularly dispersed within the bCN matrix, which further increases their suitability for oral drug delivery [30]. This as well is consistent with our finding for celecoxib being molecularly dispersed in bCN micelles, as found by solution and solid-state nuclear magnetic resonance [29]. But here, importantly, the amorphous encapsulation is confirmed also for drug combinations.

In earlier works, different ARVs were encapsulated in various (mainly polymeric) nanocarriers especially integrase strand transfer inhibitors i.e. dolutegravir, cabotegravir [39], nucleoside/nucleotide reverse transcriptase inhibitors i.e. emtricitabine, tenofovir alafenamide [3], non-nucleoside reverse transcriptase inhibitors i.e EFV, rilpivirine and protease inhibitors i.e. DRV, lopinavir with boosting agent i.e. RTV [23]. Nowacek et al [40] manufactured nanoparticles of atazanavir, EFV, and RTV (termed nanoART) by using human monocyte-derived macrophages as a carrier but these were not tested for oral delivery as they were envisioned for the targeting the central nervous system. Our strategy is substantially distinct from others that in most of cases

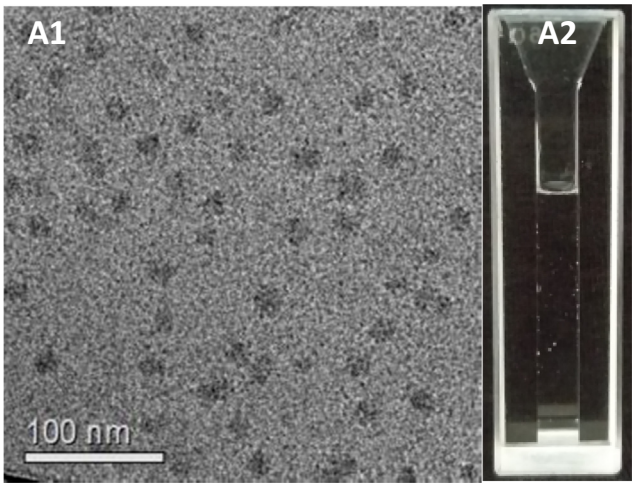

Fig. 5. (A) Cryo-TEM shows uniform bCDER micelles (1:8:6:1, protein:drugs mole ratio) after lyophilization and resuspension to a 5-fold higher concentration (50 mg mL^{-1}) than the original one. (B) The colloidal dispersion remains transparent.

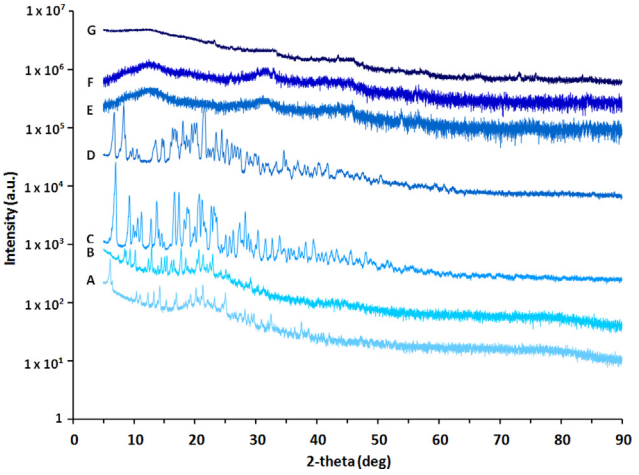

Fig. 6. Representative XRD spectra of free drugs (A to D) compared to bCN (E) and bCN with encapsulated drugs (F to G). (A) EFV, (B) TRP, (C) DRV, (D) RTV (E) bCN micelles, (F) bCTE, and (G) bCDER. Measurements clearly show no peaks of drugs in the presence of bCN micelles indicating encapsulated drugs in an amorphous form.

encapsulate one single drug, as we demonstrate in this work the co-encapsulation, with almost 100% efficiency, of double and triple ARV combinations. As stressed above, TRP:EFV was utilized to optimize the process conditions and the bCN:drugs ratio to maximize encapsulation, DRV:EFV:RTV is an ARV combination administered once daily in healthy volunteers in the amount of 900, 600 and 100 mg respectively [41].

3.3. Production and characterization of gastro-resistant Nanoparticle-in-Microparticle Delivery Systems

As previously shown, upon oral administration, protease inhibitors initially undergo dissolution in the stomach and reprecipitate in the small intestine [22,23]. To assess this behavior for all the ARVs used in this study, free drug combinations of TRP:EFV and DRV:EFV:RTV (composition as in Table 1) were dissolved in 0.001 M HCl solution of pH 2.0. As seen in Fig. 7A1, B1, in both experiment drugs dissolved and formed solutions that were transparent to both the naked eye and under the LM. Upon pH increase to pH 6.8 (this mimics *in vitro* the transit of the drugs from the stomach to the small intestine), we noticed the presence of large drugs particles of several microns in size (Fig. 7A2, B2). These results indicate that these pH-dependent drugs undergo dissolution at low pH and then, upon neutralization, they re-precipitate in the form of microparticles. This phenomenon was demonstrated *in vivo* where DRV/RTV pure nanoparticles administered to rats by the oral route showed very similar pharmacokinetics to unprocessed drugs [23]. To prevent this, protease inhibitor nanoparticles need to be encapsulated within gastro-resistant capsules that release the drug locally in the small intestine [22,23,42].

Eudragit® L100, a polyanion random copolymer of methyl methacrylate and methacrylic acid (1:1 M ratio), is extensively used as a film-coating pharmaceutical excipient for improving the oral delivery of ARVs and other small-molecule drugs and proteins [22]. This copolymer is poorly soluble under the gastric pH conditions and freely soluble at the intestinal pH. Thus, microencapsulation within Eudragit® L100 is a simple, scalable and translatable approach to protect the bCN from degradation and minimize the release of the ARVs in the stomach [43]. Once in the small intestine, this copolymer is anticipated to undergo dissolution, releasing the encapsulated ARVs from the drug-loaded micelles [22]. To ensure the efficient encapsulation of the drug-loaded bCN micelles in the macroparticles and maximize the yield,

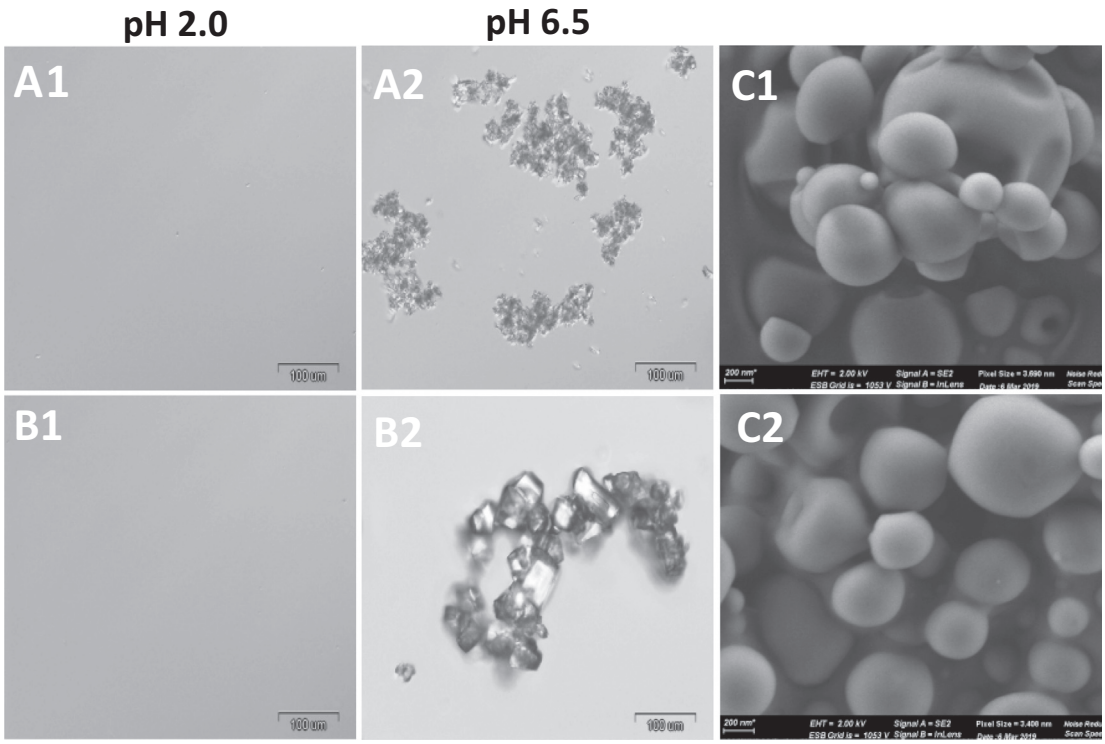

Fig. 7. LM micrographs of free drug combinations (A1) TPV:EFV and (B1) DRV:EFV:RTV showing dissolution occur at acidic pH 2.0 and (A2) TPV:EFV and (B2) DRV:EFV:RTV showing reprecipitation at neutral pH 6.5. Cuvettes showing appearance of dispersion in both the conditions. (C) HR-SEM micrographs of (C1) EbCTE and (C2) EbCDER showing spherical round shape microparticles.

we used the spray-drying technology. In this framework, bCTE and bCDER dispersions were dispersed in an ethanol solution of the copolymer and spray-dried under optimized conditions as described in the experimental section. Ethanol is an optimal solvent because it is approved for pharmaceutical use and it does not affect the structure and size of the bCN micelles in a substantial manner. In addition, it does not dissolve any of the ARVs used in this study within the timeframe of the production process, thus preserving the integrity of the drug-loaded micelles. We successfully prepared microparticles for both micellar dispersions, namely EbCTE and EbCDER, having mean hydrodynamic diameter of 590 ± 90 nm and 540 ± 70 nm, respectively, as determined by DLS (Fig. 2SA). Z-potential values were −35 ± 3 mV and –38 ± 4 m V, respectively, in accordance with the negative charge provided by the carboxylic acid groups in the side-chain of Eudragit® L100 (Fig. 2SB). Taken together, size and Z-potential values suggest that the produced NiMDS will be physically stable in suspension owing to electrostatic repulsion. To gain more insight into the size and the morphology of EbCTE and EbCDER, they were examined by HR-SEM. We identified mainly a population of round-shaped, smooth-surfaced microparticles with a diameter of approximately 435 ± 55 nm for EbCTE and 470 ± 70 nm for EbCDER (Fig. 7C1, C2), confirming the successful production of NiMDS.

To confirm the integrity of the Eudragit® L100 coating around the bCN micelles, FTIR analysis of bCN, pure Eudragit® L 100 and the drug-free bCN microparticles was performed. bCN showed characteristic peaks of amide I and II stretching at 1646 and 1534 cm^{-1}, respectively, and at 718 cm^{-1} due to the stretching of CH_2– groups (Fig. 3S), in good agreement with the literature [44]. The spectrum of Eudragit® L100 showed the characteristic carbonyl vibrations of the ester group at 1728 cm^{-1} (Fig. 3S). In addition, peaks at 2996 and 2953 cm^{-1} due to stretching of CH_2– groups could be found in both bCN and Eudragit® L100 spectra [45,46]. Interestingly, spectra of drug-free bCN microparticles showed a peak at 1728 cm^{-1} and the decrease of bCN characteristic amide bands, which confirmed that the copolymer coated the nanoparticles.

3.4. Drug release in vitro

Eudragit® L100 coating was anticipated to prevent drugs dissolution under gastric-like pH conditions. As a proof of concept, we chose EbCDER - a combination of three clinically relevant ARVs - and its respective uncoated version (bCDER) to assess the drug release *in vitro* first under gastric-like and then intestinal-like pH conditions. This protocol mimics the transit of the dispersions along the GIT after oral administration [22,23,47]. At pH 2.0, after 1 h, bCDER showed a relatively fast release of DRV, EFV and RTV of approximately 28.0 ± 2.0%, 11.0 ± 100% and 34.0 ± 4.0%, respectively, (Fig. 8A and Table S2). Conversely, EbCDER showed a dramatic decrease in the release to 4.0 ± 0.3%, 4.0 ± 0.5% and 20.0 ± 1.0% (Fig. 8A and Table S2), respectively. These results clearly indicate that the copolymer microparticle successfully protected the micelles and limited drug release at low pH. The small amount of drug that was released might be by presence of some free drug-loaded bCN micelles/at the surface of the microparticles or in solution. At pH 6.8, the cumulative release of DRV, EFV and RTV from the uncoated (free) micelles after 4 h was 44.0 ± 3.0%, 24.0 ± 3.0% and 46.0 ± 2.0%, respectively (Fig. 8B and Table S2). With EbCDER, values were 37.0 ± 3.0%, 20.0 ± 2.0% and 39.0 ± 3.0%, for DRV, EFV and RTV, respectively (Fig. 8B and Table S2). The differences in drug release between bCDER and EbCDER under neutral conditions was not statistically significant, confirming the dissolution of the Eudragit® L100 microparticle and the release of the ARV-loaded micelles [47]. The high drug release under neutral pH is beneficial for oral drug delivery as most drugs undergo absorption in the small intestine owing to the large absorption surface area and the longer residence time with respect

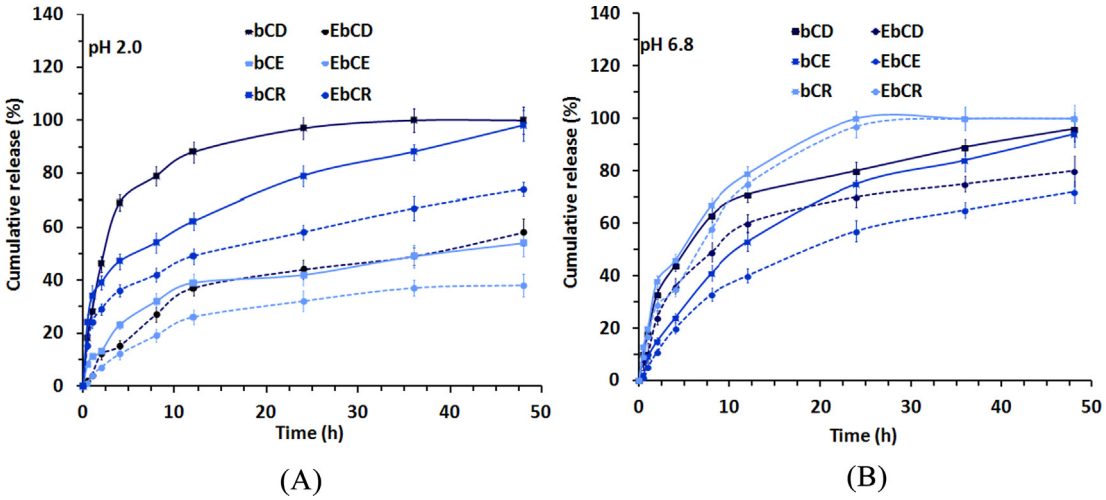

Fig. 8. DRV, EFV and RTV release profile from bCDER (solid line) and EbCDER (dotted line) under (A) gastric pH condition; pH 2.0 and (B) intestinal pH condition; pH 6.8. The results from two independent experiments are presented as mean values ± S.D.

to the stomach [33]. Overall, our results demonstrate the distinct stability and cumulative release profile of all drugs from both dispersions under gastrointestinal-like conditions with a substantial decrease at low pH. Recent work explored strategies as ligand switchable and chain responsive delivery system [48,49], imaging guided combination therapy [50] and single-wavelength near-infrared (NIR) light-triggered multifunctional micelles for combinational treatment of photothermal therapy (PTT) and photodynamic therapy (PDT) [51] to deliver hydrophobic drugs in targeted site safely, with improved therapeutic potential and lower adverse reactions.

3.5. Protection against gastric enzymes

Eudragit® L100 plays a dual role by reducing drug release and, at the same time, protecting bCN micelles from enzymatic proteolysis. To evaluate the performance of both dispersions, bCDER and its corresponding EbCDER (10 mg) were incubated in the presence of acidic protease enzyme (6 U) in simulated gastric conditions and the degradation was monitored over time. Fig. 4S depicts the pattern of bCDER degradation as a function of protease enzyme activity. After 10 min, 18% protease activity was detected, and the maximum enzyme activity has been observed at 40 min, confirming the degradation of bCN. After this time point, a reduction in enzyme activity is detected, which could be due to absence of substrate [52]. As expected, no enzymatic degradation could be recorded for EbCDER due to the efficient isolation of bCN micelles from the degradation medium. These findings confirmed that Eudragit® L100 prevents the proteolysis of drug- loaded bCN micelles under simulated gastric conditions.

4. Conclusions

Combination therapy is needed for difficult-to-treat infections because of their potency and reduced development of drug resistance. We previously introduced the use of β-casein micelles in dry form and as a colloidal dispersion as effective vehicles for oral delivery of poorly soluble drugs, using celecoxib as a model drug [29–31]. Compared to earlier research [3,39] where mainly polymers were used as a carrier for ARV drug, in the present work we reportfor the first time on successful production of, an innovative oral drug delivery system composed of double and triple ARV combinations co-encapsulated within bCN micelles and further encapsulated within Eudragit® L100 microparticles. The drug-loaded micelles were produced without any additives (e.g., surfactants), have a spherical shape and uniform size, and can successfully encapsulate high concentrations of designed combinations of hydrophobic drugs. In addition, they could undergo freeze-drying to produce stable and redispersible powders without the addition of any cryo/lyoprotectant. Further, our engineered NiMDS prevents the release of the cargos and protect the protein micelles under the acid and degradative conditions of the stomach, and are expected to release to the small intestine, which could be beneficial to increase their oral absorption and bioavailability. Overall, our results demonstrate the promising performance of this drug delivery platform to reduce the dose and the frequency of administration of ARV drugs, a crucial step to overcome the current patient-incompliant therapy. Furthermore, the use of all FDA-approved ingredients and of scalable processes remarkably increases the chances of bench-to-bedside translation. Finally, the strategy is flexible and modular, enabling the encapsulation of different qualitative and quantitative hydrophobic drug combinations.

Declaration of Competing Interest

The authors declare that they have no known competing financial interests or personal relationships that could have appeared to influence the work reported in this paper.

Acknowledgment

This work was supported by PBC-postdoctoral fellowship from the Israel Council for Higher Education and the Technion-Guangdong Fellowship. AS thanks the support of the Phyllis and Joseph Gurwin Fund for Scientific Advancement. The protease was kindly donated by Prof. Yuval Shoham (Technion, Haifa, Israel). We thank Dr. Inbal Abutbul Ionita for professional analysis of the Cryo-TEM work.

Author contribution

PSC performed most of experiments; IAI performed the Cryo-TEM work; HMH contributed to data validation; PSC, AS, DD – designed the study, analysed the data, and wrote the manuscript.

Appendix A. Supplementary data

Supplementary data to this article can be found online at https://doi.org/10.1016/j.jcis.2020.12.021.

References

[1] The global HIV/AIDS epidemic. Available from: https://www.hiv.gov/hiv-basics/overview/data-and-trends/global-statistics, 2019 (accessed on 3 May 2020).

[2] M.R. Caplan, E.S. Daar, K.C. Corado, Next generation fixed dose combination pharmacotherapies for treating HIV, Expert Opinion Pharmacother. 19 (6) (2018) 589–596, https://doi.org/10.1080/14656566.2018.1450866.

[3] J.J. Hobson, A. Al-khouja, P. Curley, D. Meyers, C. Flexner, M. Siccardi, A. Owen, C.F. Meyers, S.P. Rannard, Semi-solid prodrug nanoparticles for long-acting delivery of water-soluble antiretroviral drugs within combination HIV therapies, Nat. Commun. 10 (1) (2019), https://doi.org/10.1038/s41467-019-09354-z.

[4] C. Chu, V. Cheng, I. Hung, M. Wong, K. Chan, K. Chan, R. Kao, L. Poon, C. Wong, Y. Guan, Role of lopinavir/ritonavir in the treatment of SARS: initial virological and clinical findings, Thorax. 59 (2004) 252–256.

[5] J. Cohen, Can an anti-HIV combination or other existing drugs outwit the new coronavirus?, Science (2020), https://doi.org/10.1126/science:abb0659.

[6] H. C. Coronavirus puts drug repurposing on the fast track. 2020 Journal [2020 17 March].Available from: https://www.nature.com/articles/d41587-020-00003-1, 2020 (accessed on 17 March 2020).

[7] "Solidarity" clinical trial for COVID-19 treatments. https://www.who.int/emergencies/diseases/novel-coronavirus-2019/global-research-on-novel-coronavirus-2019-ncov/solidarity-clinical-trial-for-covid-19-treatments.

[8] M.G. Atta, S. De Seigneux, G.M. Lucas, Clinical Pharmacology in HIV Therapy, Clin. J. Am. Soc. Nephrol. 14 (3) (2019) 435–444, https://doi.org/10.2215/CJN.02240218.

[9] X. Zhang, Anti-retroviral drugs: current state and development in the next decade, Acta. Pharm. Sin. B. 8 (2) (2018) 131–136, https://doi.org/10.1016/j.apsb:2018.01.012.

[10] N. Paengsai, G. Jourdain, N. Salvadori, A. Tantraworasin, J.Y. Mary, T.R. Cressey, R. Chaiwarith, C. Bowonwatanuwong, S. Bhakeecheep, N. Kosachunhanun, Recommended first-line antiretroviral therapy regimens and risk of diabetes mellitus in HIV-infected adults in resource-limited settings, in Open Forum Infect. Dis. 2019. Oxford University Press US.

[11] WHO model lists of essential medicines. https://www.who.int/medicines/publications/essentialmedicines/en/, 2019 (accessed on 12 May 2020).

[12] D.A. Cooper, D.V. Cordery, R. Zajdenverg, K. Ruxrungtham, K. Arastéh, F. Bergmann, J.L. de Andrade Neto, J. Scherer, R.L. Chaves, P. Robinson, Tipranavir/ritonavir (500/200 mg and 500/100 mg) was virologically non-inferior to lopinavir/ritonavir (400/100 mg) at week 48 in treatment-naïve HIV-1-infected patients: a randomized, multinational, multicenter trial, Plos One. 11 (2016) e0144917.

[13] A. Tseng, C.A. Hughes, J. Wu, J. Seet, E.J. Phillips, Cobicistat versus ritonavir: similar pharmacokinetic enhancers but some important differences, Ann. Pharmacother. 51 (2017) 1008–1022.

[14] E.D. Deeks, Cobicistat: a review of its use as a pharmacokinetic enhancer of atazanavir and darunavir in patients with HIV-1 infection, Drugs. 74 (2014) 195–206.

[15] C. Marzolini, S. Gibbons, S. Khoo, D. Back, Cobicistat versus ritonavir boosting and differences in the drug–drug interaction profiles with co-medications, J. Antimicrob. Chemother. 71 (7) (2016) 1755–1758, https://doi.org/10.1093/jac/dkw032.

[16] J. Navarro, A. Curran, Profile of once-daily darunavir/cobicistat fixed-dose combination for the treatment of HIV/AIDS, HIV/AIDS (Auckl). 8 (2016) 175.

[17] N. von Hentig, Clinical use of cobicistat as a pharmacoenhancer of human immunodeficiency virus therapy, HIV/AIDS (Auckl). 8 (2016) 1–16.

[18] O. Putcharoen, T. Do, A. Avihingsanon, K. Ruxrungtham, Rationale and clinical utility of the darunavir–cobicistat combination in the treatment of HIV/AIDS, Drug Des. Devel. Ther. 9 (2015) 5763–5769.

[19] R. Cristofoletti, A. Nair, B. Abrahamsson, D.W. Groot, S. Kopp, P. Langguth, J.E. Polli, V.P. Shah, J.B. Dressman, Biowaiver Monographs for Immediate Release Solid Oral Dosage Forms: Efavirenz, J. Pharm. Sci. 102 (2) (2013) 318–329, https://doi.org/10.1002/jps.23380.

[20] J. Rubbens, J. Brouwers, J. Tack, P. Augustijns, Gastrointestinal dissolution, supersaturation and precipitation of the weak base indinavir in healthy volunteers, Eur. J. Pharm. Biopharm. 109 (2016) 122–129, https://doi.org/10.1016/j.ejpb.2016.09.014.

[21] D. Law, E.A. Schmitt, K.C. Marsh, E.A. Everitt, W. Wang, J.J. Fort, S.L. Krill, Y. Qiu, Ritonavir–PEG 8000 amorphous solid dispersions: in vitro and in vivo evaluations, J. Pharm. Sci. 93 (2004) 563–570.

[22] J.C. Imperiale, P. Nejamkin, M.J. del Sole, C. E. Lanusse, A. Sosnik, Novel protease inhibitor-loaded Nanoparticle-in-Microparticle Delivery System leads to a dramatic improvement of the oral pharmacokinetics in dogs, Biomaterials 37 (2015) 383–394, https://doi.org/10.1016/j.biomaterials.2014.10.026.

[23] R. Augustine, D.L. Ashkenazi, R.S. Arzi, V. Zlobin, R. Shofti, A. Sosnik, Nanoparticle-in-microparticle oral drug delivery system of a clinically relevant darunavir/ritonavir antiretroviral combination, Acta Biomater. 74 (2018) 344–359, https://doi.org/10.1016/j.actbio.2018.04.045.

[24] A. Sosnik, D.A. Chiappetta, Á.M. Carcaboso, Drug delivery systems in HIV pharmacotherapy: what has been done and the challenges standing ahead, J. Control. Release. 138 (2009) 2–15.

[25] J. Neves, B. Sarmento, A. Sosnik, Biomedical engineering approaches for HIV/AIDS Prophylaxis, diagnostics and therapy, Adv. Drug Deliv. Rev. 103 (2016) 1.

[26] A. Sosnik, R. Augustine, Challenges in oral drug delivery of antiretrovirals and the innovative strategies to overcome them, Adv. Drug Deliv. Rev. 103 (2016) 105–120, https://doi.org/10.1016/j.addr.2015.12.022.

[27] I. Portnaya, U. Cogan, Y.D. Livney, O. Ramon, K. Shimoni, M. Rosenberg, D. Danino, Micellization of Bovine β-Casein Studied by Isothermal Titration Microcalorimetry and Cryogenic Transmission Electron Microscopy, J. Agric. Food Chem. 54 (15) (2006) 5555–5561, https://doi.org/10.1021/jf060119c.

[28] C. Moitzi, I. Portnaya, O. Glatter, O. Ramon, D. Danino, Effect of Temperature on Self-Assembly of Bovine β-Casein above and below Isoelectric pH. Structural Analysis by Cryogenic-Transmission Electron Microscopy and Small-Angle X-ray Scattering, Langmuir 24 (7) (2008) 3020–3029, https://doi.org/10.1021/la702802a.

[29] M. Bachar, A. Mandelbaum, I. Portnaya, H. Perlstein, S. Even-Chen, Y. Barenholz, D. Danino, Development and characterization of a novel drug nanocarrier for oral delivery, based on self-assembled β-casein micelles, J. Control. Release. 160 (2) (2012) 164–171, https://doi.org/10.1016/j.jconrel.2012.01.004.

[30] T. Turovsky, R. Khalfin, S. Kababya, A. Schmidt, Y. Barenholz, D. Danino, Celecoxib encapsulation in β-casein micelles: structure, interactions, and conformation, Langmuir. 31 (2015) 7183–7192.

[31] H. Perlstein, T. Turovsky, P. Gimeson, R. Cohen, A. Rubinstein, D. Danino, Y. Barenholz, Thermotropic behavior of celecoxib-loaded beta-casein micelles: relevance to the improved bioavailability, Eur. J. Nanomed. 7 (2015) 303–312.

[32] A. Banerjee, J. Qi, R. Gogoi, J. Wong, S. Mitragotri, Role of nanoparticle size, shape and surface chemistry in oral drug delivery, J. Control. Release. 238 (2016) 176–185, https://doi.org/10.1016/j.jconrel.2016.07.051.

[33] B. Homayun, X. Lin, H.-J. Choi, Challenges and recent progress in oral drug delivery systems for biopharmaceuticals, Pharmaceutics. 11 (2019) 129.

[34] G.A. Ruiz, M. Opazo-Navarrete, M. Meurs, M. Minor, G. Sala, M. van Boekel, M. Stieger, A.E.M. Janssen, Denaturation and in Vitro Gastric Digestion of Heat-Treated Quinoa Protein Isolates Obtained at Various Extraction pH, Food Biophys. 11 (2) (2016) 184–197, https://doi.org/10.1007/s11483-016-9429-4.

[35] D. Danino, Cryo-TEM of soft molecular assemblies, Curr. Opin. Colloid Interface Sci. 17 (6) (2012) 316–329, https://doi.org/10.1016/j.cocis.2012.10.003.

[36] A. Sosnik, K.P. Seremeta, Advantages and challenges of the spray-drying technology for the production of pure drug particles and drug-loaded polymeric carriers, Adv. Colloid Interface Sci. 223 (2015) 40–54, https://doi.org/10.1016/j.cis.2015.05.003.

[37] W. Abdelwahed, G. Degobert, S. Stainmesse, H. Fessi, Freeze-drying of nanoparticles: formulation, process and storage considerations, Adv. Drug Deliv. Rev. 58 (2006) 1688–1713.

[38] B. Dutta, K. Barick, G. Verma, V. Aswal, I. Freilich, D. Danino, B. Singh, K. Priyadarsini, P. Hassan, PEG coated vesicles from mixtures of Pluronic P123 and l-α-phosphatidylcholine: structure, rheology and curcumin encapsulation, Phys. Chem. Chem. Phys. 19 (2017) 26821–26832.

[39] A.R. Kirtane, O. Abouzid, D. Minahan, T. Bensel, A.L. Hill, C. Selinger, A. Bershteyn, M. Craig, S.S. Mo, H. Mazdiyasni, C. Cleveland, J. Rogner, Y.-A. Lee, L. Booth, F. Javid, S.J. Wu, T. Grant, A.M. Bellinger, B. Nikolic, A. Hayward, L. Wood, P.A. Eckhoff, M.A. Nowak, R. Langer, G. Traverso, Development of an oral once-weekly drug delivery system for HIV antiretroviral therapy, Nat. Commun. 9 (1) (2018), https://doi.org/10.1038/s41467-017-02294-6.

[40] A.S. Nowacek, JoEllyn McMillan, R. Miller, A. Anderson, B. Rabinow, H.E. Gendelman, Nanoformulated Antiretroviral Drug Combinations Extend Drug Release and Antiretroviral Responses in HIV-1-Infected Macrophages: Implications for NeuroAIDS Therapeutics, J. Neuroimmune Pharmacol. 5 (4) (2010) 592–601, https://doi.org/10.1007/s11481-010-9198-7.

[41] G.H. Soon, P. Shen, E.-L. Yong, P. Pham, C. Flexner, L. Lee, Pharmacokinetics of Darunavir at 900 Milligrams and Ritonavir at 100 Milligrams Once Daily when Coadministered with Efavirenz at 600 Milligrams Once Daily in Healthy Volunteers, Antimicrob. Agents Chemother. 54 (7) (2010) 2775–2780, https://doi.org/10.1128/AAC.01564-09.

[42] B. Xu, W. Zhang, Y. Chen, Y. Xu, B.o. Wang, L.i. Zong, Eudragit® L100-coated mannosylated chitosan nanoparticles for oral protein vaccine delivery, Int. J. Biol. Macromol. 113 (2018) 534–542, https://doi.org/10.1016/j.ijbiomac.2018.02.016.

[43] J.S. Kim, J.H. Park, S.C. Jeong, D.S. Kim, A.M. Yousaf, F.U. Din, J.O. Kim, C.S. Yong, Y.S. Youn, K.T. Oh, S.G. Jin, H.-G. Choi, Novel revaprazan-loaded gelatin microsphere with enhanced drug solubility and oral bioavailability, J. Microencapsul. 35 (5) (2018) 421–427, https://doi.org/10.1080/02652048.2018.1515997.

[44] H. Farrell Jr, E. Wickham, J. Unruh, P. Qi, P. Hoagland, Secondary structural studies of bovine caseins: temperature dependence of β-casein structure as analyzed by circular dichroism and FTIR spectroscopy and correlation with micellization, Food Hydrocoll. 15 (2001) 341–354.

[45] A. Ptiček Siročić, L. Kratofil Krehula, Z. Katančić, Z. Hrnjak-Murgić, Characterization of casein fractions–Comparison of commercial casein and casein extracted from cow's milk, Chem. Biochem. Eng. 30 (2016) 501–509.

[46] M. Sharma, V. Sharma, A.K. Panda, D.K. Majumdar, Development of enteric submicron particle formulation of papain for oral delivery, Int. J. Nanomedicine. 6 (2011) 2097.
[47] S. Thakral, N.K. Thakral, D.K. Majumdar, Eudragit®: a technology evaluation, Expert Opin. Drug. Deliv. 10 (1) (2013) 131–149, https://doi.org/10.1517/17425247.2013.736962.
[48] Y. Ding, J. Liu, Y. Zhang, X. Li, H. Ou, T. Cheng, L. Ma, Y. An, J. Liu, F. Huang, Y. Liu, L. Shi, Nanoscale Horiz. 4 (2019) 658–666.
[49] X. Ding, C. Hong, G. Zhang, J. Liu, H. Ouyang, M. Wang, L. Dong, W. Zhang, H. Xin, X. Wang, Nanoscale Horiz. 4 (2019) 1277–1285.
[50] Z. Yang, Y. Dai, L. Shan, Z. Shen, Z. Wang, B.C. Yung, O. Jacobson, Y. Liu, W. Tang, S. Wang, L. Lin, G. Niu, P. Huang, X. Chen, Nanoscale Horiz. 4 (2019) 426–433.
[51] X. Hu, H. Tian, W. Jiang, A. Song, Z. Li, Y. Luan, Small 14 (2018) e1802994.
[52] N. George, P.S. Chauhan, V. Kumar, N. Puri, N. Gupta, Approach to ecofriendly leather: characterization and application of an alkaline protease for chemical free dehairing of skins and hides at pilot scale, J. Cleaner Prod. 79 (2014) 249–257.